Bulletin of Engineering Geology and the Environment (2024) 83:391
https://doi.org/10.1007/s10064-024-03886-5

ORIGINAL PAPER

Rock abrasiveness prediction based on multi-source physical, mechanical and mineralogical properties

Yun Wu[1] · Long-Chuan Deng[1,2] · Xiao-Zhao Li[1] · Li-Yuan Yu[1] · Jiang-Feng Liu[1] · Jian Lin[3]

Received: 17 March 2024 / Accepted: 26 August 2024

Abstract

Rock abrasiveness is a vital parameter affecting cutter wear, tunneling efficiency, and cost budgeting during mechanical excavation. The Cerchar abrasivity index (CAI), a suggested standard parameter to characterize the rock abrasiveness, can be obtained through the laboratory test. Understanding the correlations between the CAI and physical, mechanical, and mineralogical properties helps to precisely evaluate the cutter wear and improve the excavation efficiency. In this paper, correlations between CAI and 17 commonly used rock parameters were established for 27 groups of rock samples collected from China using simple and multiple regression methods. Based on the Pearson correlation coefficient (PCC) results, the possibility of linear relationships between CAI and physical, mechanical, and mineralogical parameters of rock samples was analyzed for determining the appropriate model. Subsequently, simple linear regression and Boltzmann models were developed based on physical and mechanical parameters. The model based on porosity showed excellent forecasting performance over other models. Through the analysis on the coefficient of determination (R^2) value, a better multiregression model ($R^2 = 0.92$) based on the mechanical parameters was obtained. However, a more feasible model ($R^2 = 0.91$) based on the thermal conductivity, diffusion coefficient, elastic modulus, and Rock Abrasivity Index (RAI) was also suggested, considering the simplicity and period of parameter measurement. After the classification of rock types, the linear correlations strengthened significantly, especially for the mineralogical properties. The CAI showed a linear correlation with equivalent quartz content (EQC) and RAI for the granite and sandstone, while the quartz content (Q) still showed no relation with CAI. The results can provide a reference for evaluating the abrasive properties of rock during the mechanical excavation process.

Keywords Cerchar abrasivity index(CAI) · Mineralogical properties · Physical and mechanical properties · Prediction model

Introduction

Mechanical excavation has become the mainstream technology for underground construction, and has been widely applied to river crossings, road tunnels, metro tunnels, mining projects and so on (Deng et al. 2022a, b, c). The cutter is a crucial component of the excavating machinery and contacts the rocks directly. As a result of the thrust and torque, the cutter contacts, penetrates, squeezes, and abrades the rocks, and eventually the cutter wears out until failed (Sun et al. 2023). Notably, wear is the progressive loss of material from the cutting tools. Four wear mechanisms comprising adhesive wear, abrasion, surface fatigue, and tribochemical reaction are proposed, moreover, the adhesive wear is highlighted as the most important wear mechanism caused by the relative sliding motion at the cutter-rock interface (Majeed and Abu Bakar 2016). Hence, rock abrasivity is a necessary parameter to precisely evaluate the lifetime of the cutters and accurately calculate the construction costs in the mining and tunnelling industries.

Cutter wear is one of the remarkable results of rock-machine interaction, which is related to the rock mass,

✉ Long-Chuan Deng
dg21290027@smail.nju.edu.cn

1 State Key Laboratory of Intelligent Construction and Healthy Operation & Maintenance of Deep Underground Engineering, China University of Mining and Technology, Xuzhou 221116, Jiangsu, China

2 School of Earth Sciences and Engineering, Nanjing University, Nanjing 210023, Jiangsu, China

3 Anhui Province Key Laboratory of Intelligent Geotechnics and Disaster Prevention, Anhui Jianzhu University, Hefei 230601, Anhui, China

Published online: 09 September 2024

tunnelling rig, and working process (Thuro and Plinninger 2003). Objective factors including the tunnelling rig and working process can be controlled and optimized ahead of the construction period. Rock mass state, an unexpected factor, is hard to be changed along the tunnel. Rocks with high abrasivity encountered during tunnelling increase the degree of cutter wear and the frequency of replacement, consequently decreasing tunnelling efficiency and increasing construction cost. Typically, the time and economic costs caused by cutter replacement account for about 1/3 of the overall construction costs in the shield tunnelling (Wang et al. 2017; Yu et al. 2021). Cutter life is overwhelmingly determined by the rock abrasivity. Thus, understanding the rock abrasivity is extremely difficult since it is related to a variety of complex factors such as physics, mechanics, and mineralogy (Er and Tuğrul et al. 2016). Some profound insights, such as the prediction of rock abrasivity based on multi-source parameters, are still worth investigating.

Many test methods have been proposed and developed to identify the rock abrasivity, each measurement method has its deficiencies and application limitations (Rostami et al. 2014). Cerchar abrasiveness test suggested by the International Society of Rock Mechanics (ISRM) is one of the most widely used rock abrasion tests (Alber et al. 2014). The effects of various factors on Cerchar abrasivity index (CAI) have been investigated in relevant literature (Ozdogan et al. 2018; Capik and Yilmaz 2017; Majeed and Abu Bakar 2016; He et al. 2016; Moradizadeh et al. 2016; Deliormanli 2012; Zhang et al. 2021; Ko et al. 2016; Zhang et al. 2020). Specifically, mineral composition, grain shape and size, and the physical and mechanical properties of rocks have a significant effect on the rock abrasiveness. However, it is not clear which parameter controls the rock abrasion. The relationship between the rock abrasivity and its factors is more controversial, both linear as well as non-linear relationships have been reported (Rostami et al. 2014; Torrijo et al. 2018; Moradizadeh et al. 2013). Moreover, Quartz content (Q), equivalent quartz content (EQC), Rock Abrasivity Index (RAI), uniaxial compressive strength (UCS), longitudinal wave velocity, grain size, density, elastic modulus (E), and Poisson's ratio, etc., have historically been determined to evaluate and predict the CAI. Notably, previous studies have assessed rock abrasivity from limited aspects of physical, mechanical, and mineralogical properties. Therefore, prediction of rock abrasivity based on multi-source physical, mechanical, and mineralogical properties is meaningful to evaluate the cutter life and understand the relevance between rock abrasivity and factors.

In this paper, the JHC01 rock abrasion servo system was used for an abrasion test on different rock samples. At the same time, a series of physico-mechanical and microscopic tests were carried out. The relationship between the rock abrasivity and physical, mechanical, and mineralogical properties were investigated. In addition, rock abrasivity prediction model was established based on the relationships between these properties and CAI using simple regression and multi regression.

Experimental scheme

Sample preparation

To obtain accurate results, sedimentary, magmatic, and metamorphic rocks were considered for inclusion in the rock samples. 27 rocks from Yunnan, Sichuan, Shandong, and Gansu provinces were selected based on accessibility and commonness to study the correlation between rock abrasivity and influencing factors. As shown in Table 1, eight granites, seven sandstones, five limestones, two shales, basalt, volcanic rock, marble, carbonaceous slate, and yellow mudstone were included in the rock samples. Only two metamorphic rocks were collected as they were more difficult to be acquired. All rocks were processed into samples of specific accuracy and size for laboratory tests (Fig. 1).

Physical and mechanical tests

Mechanical properties were evaluated through tests including uniaxial compression strength (UCS), Brazilian tensile strength (BTS), and shear strength. UCS tests were performed on the prepared core samples with a length to diameter ratio of 2:1. The loading rate was about 0.5 mm/min and three samples from each rock were subjected to uniaxial compression tests. The tests were carried out using an electronic-hydraulic servo-controlled stiff press testing machine (Fig. 2) according to the method suggested by

Table 1 Basic information of studied rock samples

No.	Rock name	No.	Rock name
A1	Sichuan grey granite	A15	Yunnan beige sandstone
A2	Rust yellow granite	A16	Yunnan limestone
A3	Wulian red granite	A17	Coralreef limestone
A4	Maple leaf red granite	A18	Cyan limestone
A5	Beige granite	A19	Shandong limestone
A6	Sesame white granite	A20	Limestone
A7	Yunnan grey granite	A21	Argillaceous shale
A8	Beishan granite	A22	Gas shale
A9	Purple sandstone	A23	Basalt
A10	Yunnan cyan sandstone	A24	Volcanic rock
A11	Shandong white sandstone	A25	Marble
A12	Sichuan grey sandstone	A26	Carbonaceous slate
A13	Sichuan red sandstone	A27	Yellow mudstone
A14	Yunnan red sandstone		

Fig. 1 Processed different rock samples

ISRM (1979) and ASTM (2010). Brazilian splitting tests were conducted on a disk sample with a length to diameter ratio of 1:2 using an electronic-hydraulic servo-controlled stiff press testing machine. The tests were completed until failure occurs across the diameter axis. A loading rate of 0.1 mm/min was applied. Three samples from each rock type were used for testing and the results were averaged. The tests were also carried out according to the method suggested by Ulusay (2015) and ASTM (2010). Shear strength tests were carried out with a variable angle plate to acquire the internal friction angle and cohesion. Three prepared samples from each rock type were processed into the cubic rock with a length of 50 mm. Shear strength tests at three angles (50 °, 60 ° and 70 °) were performed using an electronic-hydraulic servo-controlled stiff press testing machine (Fig. 2). Three samples from each rock type were used for each angle and the results were averaged, indicating that nine samples were used for each rock type. A loading rate of 0.3 mm/min was applied. The results of rock mechanical tests were represented in Table 2.

Brittleness is one of the most important mechanical properties of rock. Accurate evaluation of the rock brittleness plays an important role in the underground engineering and slope stability of water conservancy and hydropower, transport, energy exploration and development, as well as the analysis of rock drillability and cutability (Li et al. 2022). All existing brittleness indexes, which can be classified into four types, i.e., methods based on mineral content, elastic deformation, energy, stress–strain (Liu et al. 2023). In this paper, brittleness index was evaluate according to the UCS and BTS (Eq. 1) (Hucka and Das 1974).

$$B = \frac{UCS}{BTS} \tag{1}$$

where B is the brittleness value; UCS is the uniaxial compressive strength, MPa; BTS is the Brazilian tensile strength, MPa;

Physical properties include density, leeb hardness, longitudinal wave velocity, transverse wave velocity, thermal conductivity, diffusion coefficient, and porosity. Longitudinal wave velocity and transverse wave velocity were measured

Fig. 2 Rock mechanics test equipment

Table 2 Mechanical test results and brittleness values of rock samples

Rock	BTS (MPa)	UCS (MPa)	φ (°)	C (kPa)	E (GPa)	ν	B
A1	5.6	156.9	47.8	27.2	54.1	0.25	28.1
A2	5.3	132.7	48.2	22.0	44.2	0.25	24.8
A3	5.0	97.5	45.7	15.0	41.0	0.23	19.6
A4	5.4	100.1	45.0	23.4	45.1	0.24	18.4
A5	5.4	140.7	46.9	22.9	43.3	0.25	26.2
A6	5.1	101.5	44.7	11.8	36.2	0.23	20.0
A7	5.6	146.3	51.2	26.1	53.3	0.26	26.1
A8	5.7	155.9	48.9	28.5	54.3	0.24	27.4
A9	5.7	121.1	37.7	13.1	25.2	0.23	21.2
A10	4.6	88.0	42.6	8.4	18.1	0.18	19.1
A11	4.9	99.4	38.3	12.4	21.6	0.19	20.4
A12	3.2	59.6	36.6	7.2	13.0	0.21	18.5
A13	3.1	60.9	37.5	7.9	13.2	0.19	19.7
A14	3.9	73.3	35.5	10.7	16.3	0.17	18.9
A15	5.3	116.9	45.4	17.0	27.1	0.29	22.3
A16	5.8	88.9	37.4	15.4	30.9	0.20	15.4
A17	1.5	7.6	26.7	6.2	9.8	0.11	5.1
A18	5.1	104.9	42.8	16.6	32.6	0.18	20.7
A19	5.3	96.8	44.1	15.2	30.7	0.19	18.3
A20	5.7	116.8	39.2	14.2	30.0	0.20	20.3
A21	3.2	38.7	35.4	8.1	3.9	0.17	12.0
A22	6.2	117.0	36.9	16.2	30.9	0.22	18.9
A23	6.2	128.8	45.7	23.0	31.8	0.29	20.6
A24	5.1	147.7	50.4	28.2	46.5	0.26	28.9
A25	5.4	53.9	38.0	5.6	35.3	0.20	10.0
A26	6.5	87.7	37.1	15.3	24.9	0.20	13.5
A27	2.0	23.2	29.9	4.2	2.9	0.20	11.3

by an acoustic detector (RSM-SY5) (Fig. 3a). Thermal conductivity and diffusion coefficient were measured by a hot disk thermal-constants analyzer based on TPS (Fig. 3b). A leeb hardness tester was used for measuring the hardness (Fig. 3c). Five smooth and flat positions on the rock surface are selected as the testing area, then the results are averaged. The density of rocks was measured by the electronic balance (Fig. 3d) and Vernier calipers (Fig. 3e). Porosity was tested by nuclear magnetic resonance (PQ-001 Mini NMR) (Fig. 3f). All rock physical tests were measured at least three times, and the average values were used for analysis. The results of physical tests were represented in Table 3.

Mineral composition and microstructure

Understanding the mineral composition and microstructure helps to uncover the intrinsic reason of rock abrasivity. The mineral composition of rock samples was measured by a Rigaku Dmax Rapid II X-ray diffractometer, with a scanning speed of 3°/min and sampling interval of 0.02°. The sample used for X-ray diffraction (XRD) test is dry powder with particle size less than 200 mesh. The mineral composition of rocks can be determined by comparing the measured XRD patterns with the standard cards in the database. Quartz contributes the most to the rock abrasivity and high quartz content leads to high rock abrasivity (Capik and Yilmaz, 2017). The quartz content can be acquired through XRD analysis. Moreover, EQC was also calculated as proposed by Thuro and Plinninger (2003) (Eq. 2):

$$\mathrm{EQC} = \sum_{i=1}^{n} A_i \times R_i \tag{2}$$

where EQC is equivalent quartz content (%), A is mineral content (%), R is Rosiwal abrasiveness (%), and n is number of minerals.

RAI value can be acquired based on the results of mineral composition tests. RAI value is calculated using the following formula (Eq. 3) (Zhang et al. 2021). The results of rock mineralogical properties can be seen in Table 4.

$$\mathrm{RAI} = \frac{EQC \times UCS}{100} \tag{3}$$

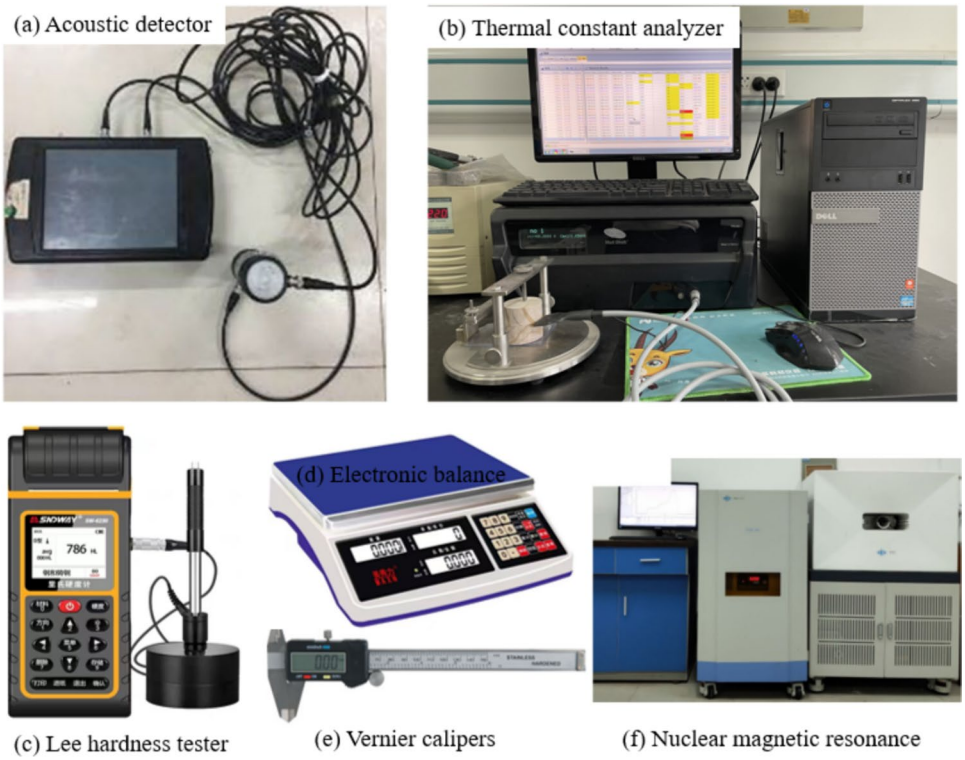

Fig. 3 Rock physical test equipment

Table 3 Physical test results of rock samples

Rock	ρ (g/cm^3)	H	V_s (m/s)	V_P (m/s)	λ (W/(m·K))	D (m^2/s)	*P* (%)
A1	2.60	824	1396	4901	4.84	2.11	1.18
A2	2.59	815	1383	4958	5.01	2.33	1.14
A3	2.59	842	1306	4757	5.16	1.61	1.64
A4	2.56	848	1389	4871	4.98	2.03	1.12
A5	2.64	792	1448	4917	4.14	2.56	1.15
A6	2.57	833	1302	4669	5.23	1.93	1.69
A7	2.68	782	1433	5282	4.03	2.99	0.87
A8	2.69	780	1453	5071	4.21	2.25	0.69
A9	2.47	638	1510	3806	4.98	1.56	8.38
A10	2.38	602	1491	3722	5.10	1.61	11.63
A11	2.46	660	1503	3765	5.96	2.04	7.86
A12	2.28	491	1494	3860	5.60	1.55	12.52
A13	2.32	516	1485	3583	6.26	1.22	13.38
A14	2.31	483	1482	3634	6.77	1.50	13.52
A15	2.45	679	1527	4438	4.82	2.36	8.13
A16	2.70	669	1673	4079	6.69	1.65	0.22
A17	1.05	12	2649	2956	8.02	0.92	56.44
A18	2.72	644	1700	4532	6.26	1.45	0.26
A19	2.74	699	1664	4670	6.52	1.79	1.24
A20	2.72	680	2016	4691	6.04	1.37	0.26
A21	2.14	411	1852	2972	7.17	1.07	12.11
A22	2.53	689	1513	4804	7.68	2.00	1.48
A23	2.53	792	1234	4910	2.51	2.79	4.72
A24	2.20	799	1362	5228	1.89	2.74	14.19
A25	2.75	566	1644	4352	6.14	1.43	0.30
A26	2.63	650	1501	3291	7.80	1.36	0.34
A27	1.98	308	2356	4173	6.61	1.16	18.08

Table 4 Results of equivalent quartz content and rock abrasivity index

No.	EQC (%)	Q (%)	RAI
A1	51.99	31.30	44.08
A2	39.68	5.70	32.93
A3	35.97	0.00	19.14
A4	36.26	0.00	18.41
A5	41.55	16.00	36.92
A6	24.66	29.20	20.29
A7	56.89	0.00	38.22
A8	45.09	17.30	42.67
A9	65.77	29.80	79.67
A10	61.68	23.30	54.27
A11	93.38	92.30	92.81
A12	68.58	66.00	40.86
A13	46.39	14.90	28.23
A14	100.00	100.00	73.35
A15	100.00	100.00	116.90
A16	1.00	0.00	0.89
A17	1.00	0.00	0.08
A18	1.00	0.00	1.05
A19	1.00	0.00	0.97
A20	1.00	0.00	1.17
A21	15.62	13.90	6.04
A22	43.47	63.10	50.85
A23	37.00	0.00	47.65
A24	46.10	0.00	68.09
A25	1.00	0.00	0.54
A26	1.00	0.00	0.88
A27	20.82	19.20	4.82

where RAI is the rock abrasion index; EQC is the equivalent quartz content; and UCS is the uniaxial compressive strength.

XRD pattern of rock samples was illustrated in Fig. 4. The main peak shape of the same rock type was basically similar, and individually there may be other stray peaks. In other words, the main mineral composition was similar for the same rock type, but there was still a slight difference. However, the peak shape and intensity of XRD pattern differed significantly for different rock types. The specific mineral contents of rock samples were represented in Table 5.

The petrological-mineralogical properties of rock samples were investigated by using a Nikon CI-POL orthogonal polarizing microscope, as illustrated in Fig. 5. Obviously, the compact granite is characterized by its medium-grained structure. Three typical minerals can be identified in the thin-section: blue feldspar, mica, and the crystal clear and colorless quartz which can be commonly seen in the rock. Sandstone is formed by weathering, stripping, and transporting rocks from the source area to accumulate in the basin. Sandstone is fine- to medium-grained, mainly consists of both clastic and filler material. The grain rounding varies from sub- to well-rounded and the grain sorting is between well- and moderately-sorted. The quartz is mainly distributed in the porous sandstone. In addition, we can also see that granite has a larger grain size than sandstone. The limestone is fine-grained and well-sorted, and composed mainly of calcite or aragonite. Shale is a sedimentary rock with thin sheets or lamellae of joints, mainly formed by clay deposits through pressure and temperature, and mixed with quartz, mica, calcite and other minerals. The basalt matrix is intergranular-interstitial cryptic, and the main minerals are feldspar, which are haphazard and interwind. The marble is medium- to coarse-grained, mainly includes the calcite. Slate is a fine-grained foliated metamorphic rock with a plate-like structure and essentially no recrystallisation. Mudstone is fine-grained sedimentary rock composed of mud and clay consolidated to a similar composition and structure as shale.

Cerchar Abrasivity Index

CAI tests were performed according to the method suggested by ISRM (Alber et al. 2014). Specifically, the specimen is fixed in the holder during the Cerchar test and the needle is placed on the specimen. The needle is an alloy steel with a tensile strength of 2 GPa, Rockwell hardness of 54–56, and a taper angle of 90°. Moreover, a weight of 7 kg is loaded on the needle moved on the specimen by the stepper motor within one minute, then the wear of needles is measured through the microscopy. Typically, 3–5 tests for the same rock are performed, and the results are averaged, then the CAI value is 10 times the average wear diameter of the steel needle. On the basis of the principle of CAI tests, a novel CAI testing equipment including rock abrasion test system, intelligent measurement system, and computer was proposed (Fig. 6a). The wear state of three typical rocks including marble, Yunnan red sandstone, and the maple leaf red granite can be seen in Fig. 6b. It can be clearly seen that the wear depth under the same load is different, indicating that there is little difference on the rock abravisity.

The CAI results were shown in Table 6. It can be seen that the CAI value of igneous rock is higher than that of sedimentary rock and metamorphic rock. The igneous rock has the maximum CAI value of 4.86, indicating very high abrasiveness according to the CAI classification suggested by ISRM (Alber et al. 2014). In contrast, the argillaceous shale has the minimum CAI value of 0.28, indicating extremely low abrasiveness. Moreover, the CAI of coralreef limestone is 0.3, which also has extremely low abrasiveness. It was generally accepted that the coralreef limestone was loose

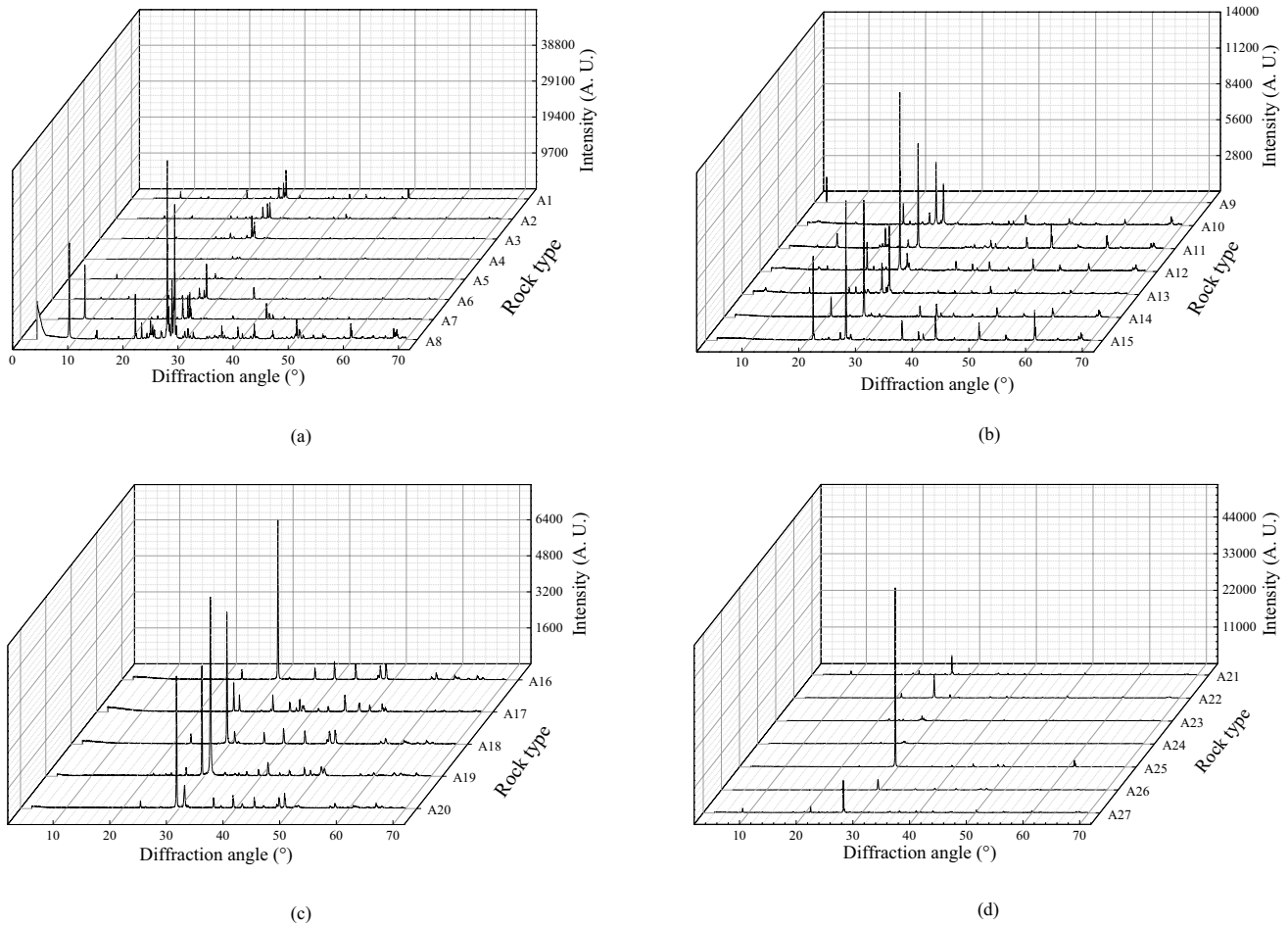

Fig. 4 XRD patterns. **a** Granite; **b** Sandstone; **c** Limestone; **d** Other rocks

and porous with good pore connectivity, and the main mineral composition was aragonite, which belonged to biogenic sedimentary rock. The real scratch length between the steel needle and coralreef limestone was less than 10 mm due to the high porosity, consequently the value of CAI was small. In summary, the magmatic rock has high abrasiveness, consequently the disc cutter wears seriously when excavating in these stratums.

Statistical analysis models for predicting CAI

Linear analysis

Pearson correlation coefficient (PCC) is advantageous for determining the positive and negative linear correlations between two characteristic variables (Tian and Su 2023), as shown in (Eq. 4). PCC ranges between − 1 and 1, where − 1 indicates a completely inverse correlation, 1 indicates a completely positive relationship, and 0 indicates no linear relationship between the two variables. PCC has a more comprehensive ability to determine the data correlation than other linear correlation coefficients such as the Euclidean distance and Jaccard distance. However, PCC does not behave significantly for the non-linear relationship, even if there is some correspondence between the two variables, which is a drawback that PCC cannot overcome.

$$r = \frac{p\sum_{i=1}^{p} x_i y_i - \sum_{i=1}^{p} x_i \sum_{i=1}^{p} y_i}{\sqrt{p\sum_{i=1}^{p} x_i^2 - (\sum_{i=1}^{p} x_i)^2}\sqrt{p\sum_{i=1}^{p} y_i^2 - (\sum_{i=1}^{p} y_i)^2}} \quad (4)$$

where r is PCC, x_i is the influential variable, y_i is the target value, and p is the total number of samples.

Three types of data including physical, mechanical, and mineralogical aspects were input parameters for the PCC. Specifically, as shown in Table 7, seven physical parameters (density, leeb hardness, longitudinal wave velocity, transverse wave velocity, thermal conductivity,

Table 5 Mineral composition of rock samples

No.	Quartz (%)	Albite (%)	Anorthite (%)	Orthoclase (%)	Annite (%)	Phlogopite (%)	Muscovite (%)	Calcite (%)	Aragonite (%)	Other (%)
A1	31.3	55.2	0	0	13.5	0	0	0	0	0
A2	5.7	51.7	0	0	0	42.6	0	0	0	0
A3	0	19.2	76.3	0	0	0	0	0	0	4.5
A4	0	34.5	0	62.3	0	0	0	0	0	3.2
A5	16	68.2	0	0	15.8	0	0	0	0	0
A6	29.2	68.7	0	0	2.1	0	0	0	0	0
A7	0	13.8	57.3	0	0	28.9	0	0	0	0
A8	17.3	73.3	0	0	5.4	0	0	0	0	4
A9	29.8	70.2	0	0	0	0	0	0	0	0
A10	23.3	76.7	0	0	0	0	0	0	0	0
A11	92.3	0	0	0	0	0	0	0	0	7.7
A12	66	34	0	0	0	0	0	0	0	0
A13	14.9	85.1	0	0	0	0	0	0	0	0
A14	100	0	0	0	0	0	0	0	0	0
A15	100	0	0	0	0	0	0	0	0	0
A16	0	0	0	0	0	0	0	100	0	0
A17	0	0	0	0	0	0	0	0	100	0
A18	0	0	0	0	0	0	0	100	0	0
A19	0	0	0	0	0	0	0	100	0	0
A20	0	0	0	0	0	0	0	100	0	0
A21	13.9	0	0	0	0	0	86.1	0	0	0
A22	63.1	0	0	0	0	0	0	36.9	0	0
A23	0	54.1	45.9	0	0	0	0	0	0	0
A24	0	13.8	82.3	0	0	0	0	0	0	3.9
A25	0	0	0	0	0	0	0	100	0	0
A26	0	0	0	0	0	0	0	100	0	0
A27	19.2	0	0	0	0	0	80.8	0	0	0

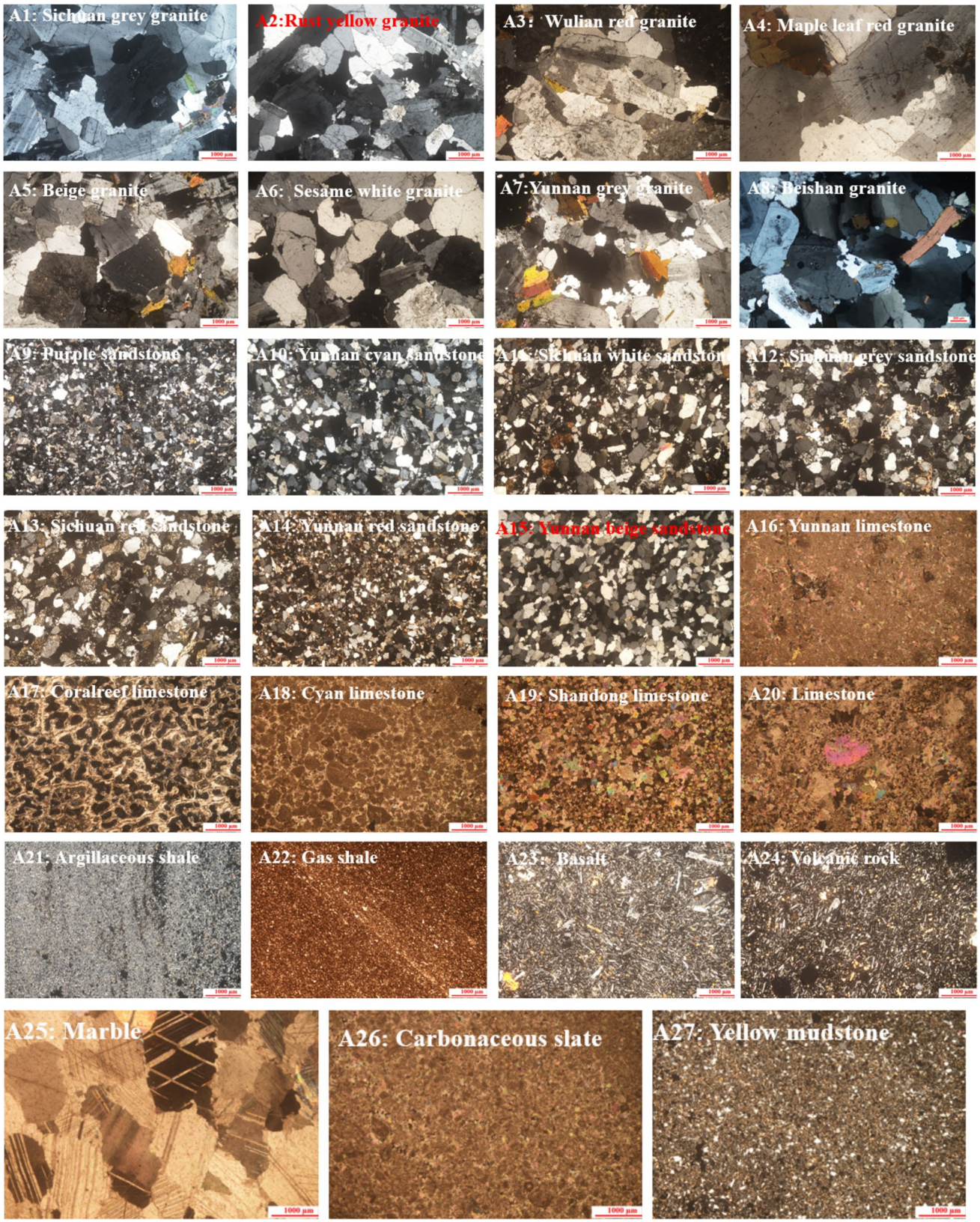

Fig. 5 The petrographic observation of rock samples

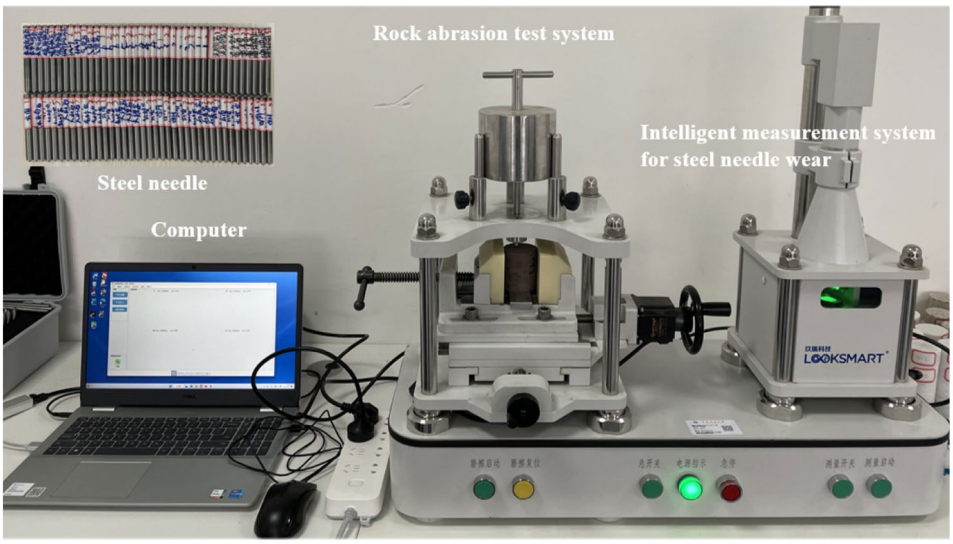

(a)

(b)

Fig. 6 CAI measurement equipment and the wear state. **a** CAI measurement equipment; **b** Typical samples after measurement

Table 6 Results of cerchar abrasiveness index (CAI)

No.	CAI	Standard deviations	No.	CAI	Standard deviations
A1	4.17	0.29	A15	3.17	0.18
A2	4.11	1.04	A16	1.18	0.09
A3	3.40	0.31	A17	0.30	0.17
A4	3.78	0.42	A18	1.26	0.15
A5	4.09	0.39	A19	1.30	0.09
A6	3.41	0.61	A20	1.17	0.27
A7	4.73	0.39	A21	0.28	0.03
A8	4.39	0.45	A22	1.89	0.24
A9	2.06	0.36	A23	3.58	0.27
A10	1.92	0.43	A24	4.86	0.43
A11	2.23	0.44	A25	1.58	0.48
A12	1.33	0.19	A26	0.77	0.07
A13	1.27	0.34	A27	0.63	0.19
A14	0.97	0.21			

diffusion coefficient, and porosity), seven mechanical parameters (uniaxial compressive strength, Brazilian tensile strength, elastic modulus, Poisson's ratio, internal friction angle, cohesion, and brittleness), and three mineralogical parameters (rock abrasion index, equivalent quartz content, and quartz content) were used to predict the CAI value. The PCC values for 17 input parameters are shown in Fig.7. There are strong positive linear correlations between CAI and longitudinal wave velocity, diffusion coefficient, UCS, internal friction angle, cohesion, elastic modulus, Poisson's ratio, and brittleness, with a PCC value greater than 0.8. The negative correlations between the CAI and transverse wave velocity and thermal conductivity are high. Notably, there are minimal linear relationships between the CAI and density, porosity, BTS, EQC, Q, and RAI. It is evidently accepted that there is maximum linear relationship between CAI and internal friction angle and diffusion coefficient.

Table 7 Feature sets of physico-mechanical and CAI parameters

Variable types	Variables	Feature set
Physical parameters	Density (g/cm^3)	X1
	Leeb hardness	X2
	Transverse wave velocity (m/s)	X3
	Longitudinal wave velocity (m/s)	X4
	Thermal conductivity (W/m·K)	X5
	Diffusion coefficient (m^2/s)	X6
	Porosity (%)	X7
Mechanical parameters	Brazilian tensile strength (MPa)	X8
	Uniaxial compressive strength (MPa)	X9
	Internal friction angle (°)	X10
	Cohesion (kPa)	X11
	Elastic modulus (GPa)	X12
	Poisson's ratio	X13
	Brittleness	X14
Mineralogical parameters	Equivalent quartz content (%)	X15
	Quartz content (%)	X16
	Rock abrasion index	X17
Abrasivity parameters	Cerchar abrasivity index	X18

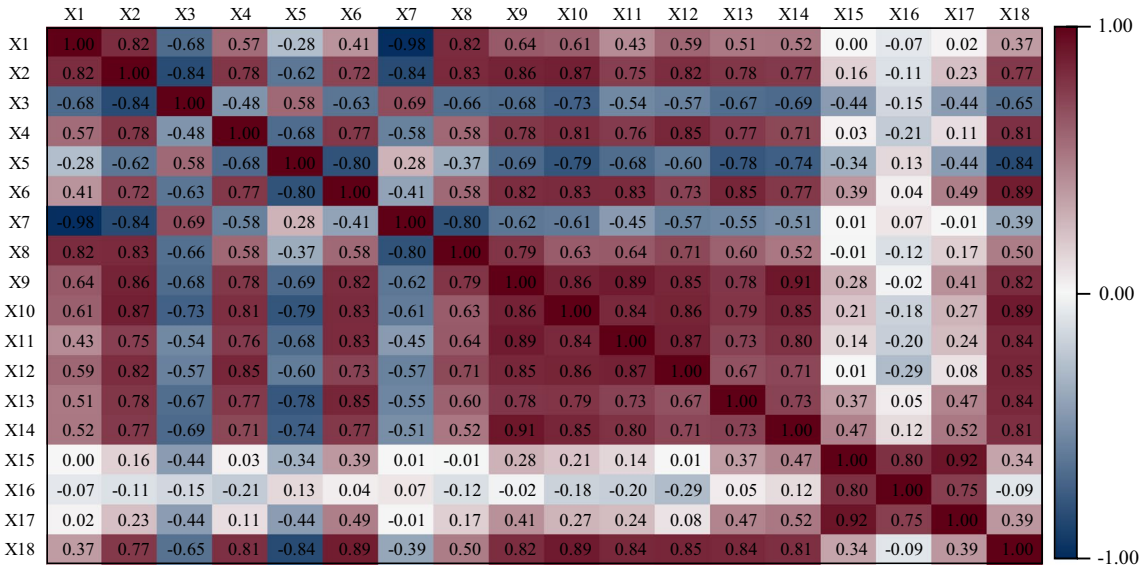

Fig. 7 Pearson correlation coefficient diagram

Simple regression

Simple regression was used to evaluate the relationship between CAI and other parameters. Three types of correlations including positive, negative linear, and nonlinear correlations were obtained based on PCC results. CAI was negatively correlated with the transverse wave velocity (Fig. 8c) and thermal conductivity (Fig. 8e) for the physical properties. CAI was positively correlated with leeb hardness (Fig. 8b), longitudinal wave velocity (Fig. 8d), and diffusion coefficient (Fig. 8f) for the physical properties. The coefficient of determination (R^2) between CAI and diffusion

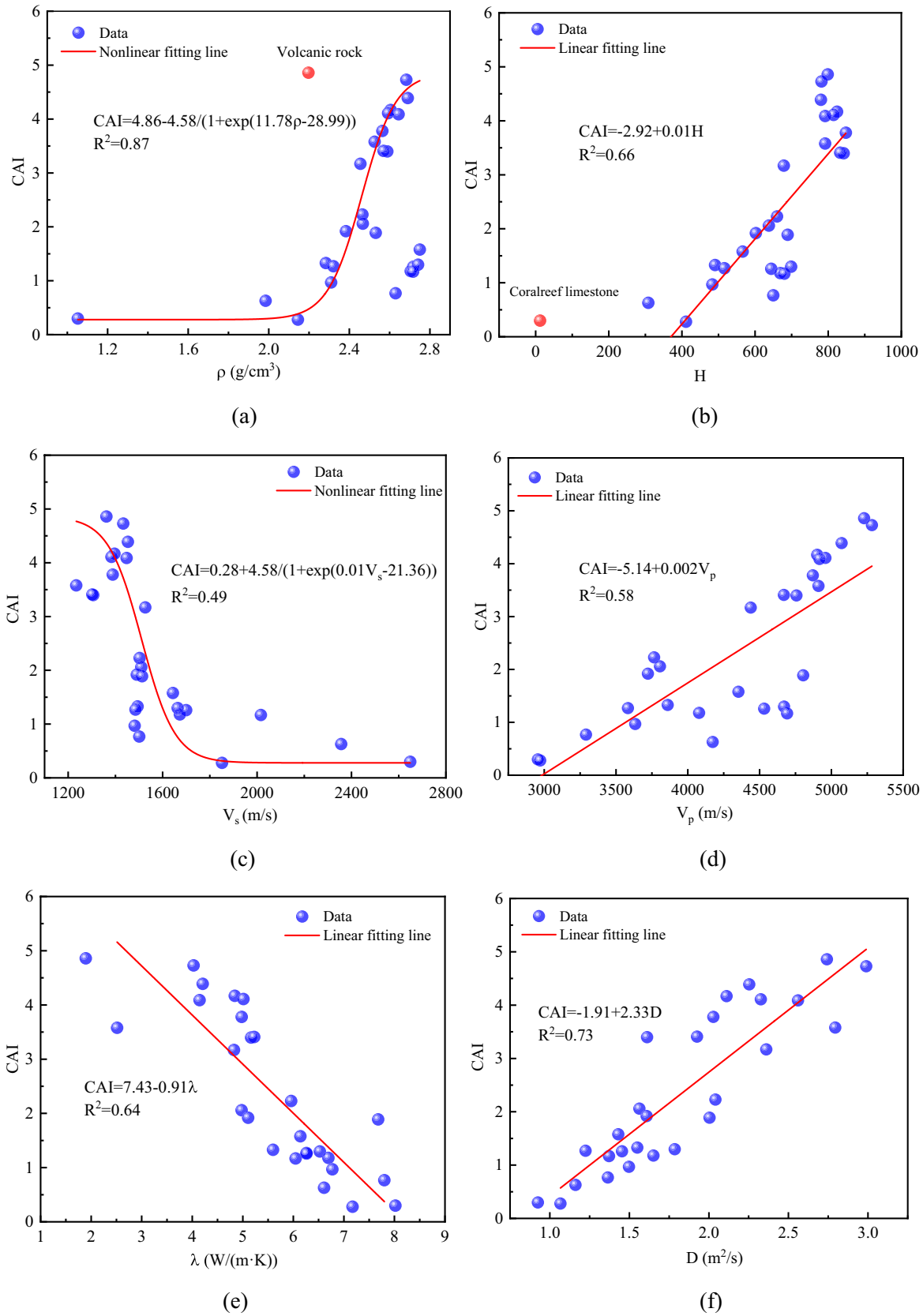

Fig. 8 The relationship between the CAI and rock properties. **a** Density; **b** Leeb hardness; **c** S-wave velocity; **d** P-wave velocity; **e** Thermal conductivity; **f** Diffusion coefficient; **g** Porosity; **h** BTS; **i** UCS; **j** Internal friction angle; **k** Cohesion; **l** Elastic modulus; **m** Poisson's ratio; **n** Brittleness; **o** EQC; **p** Q; **q** RAI

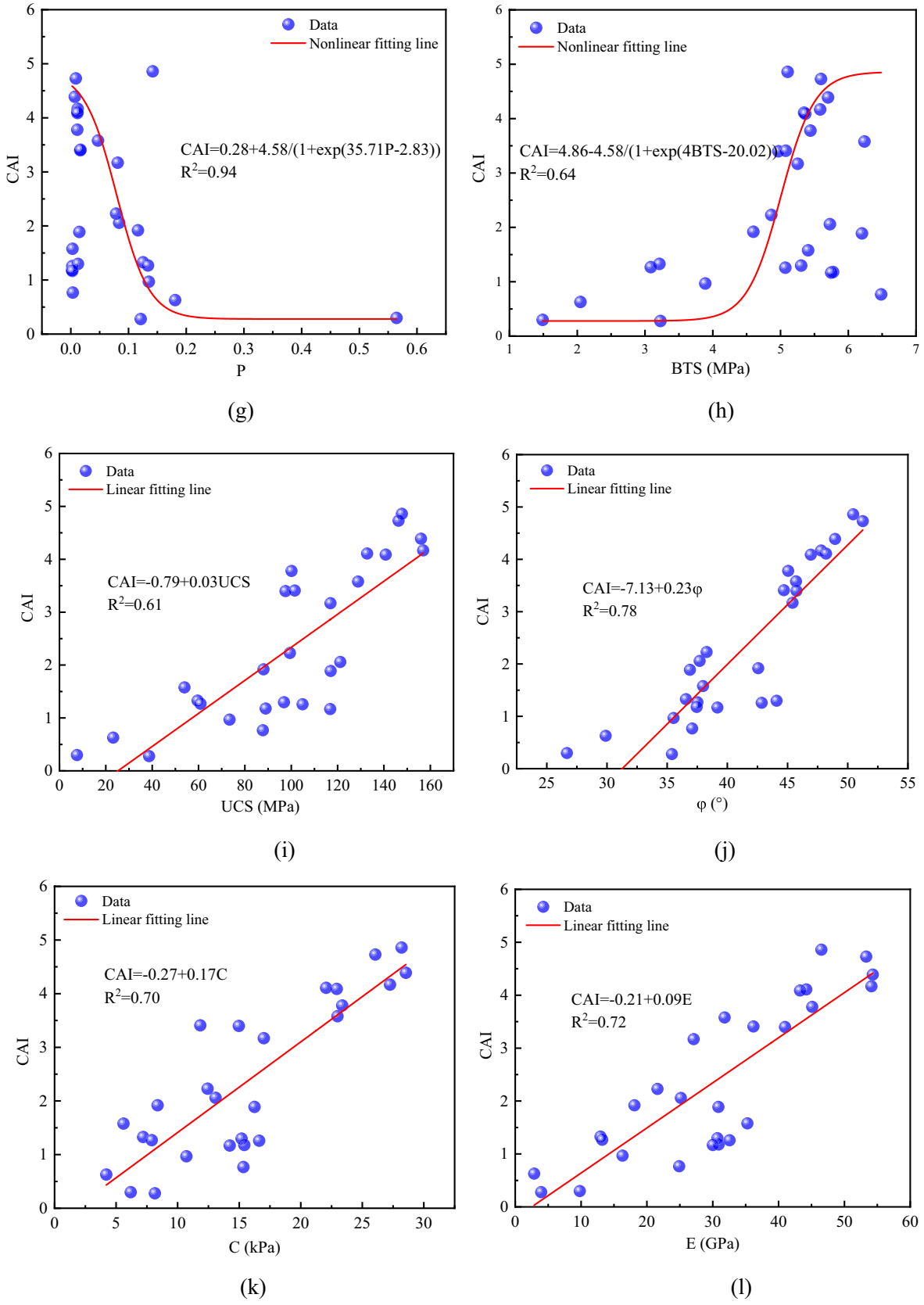

Fig. 8 (continued)

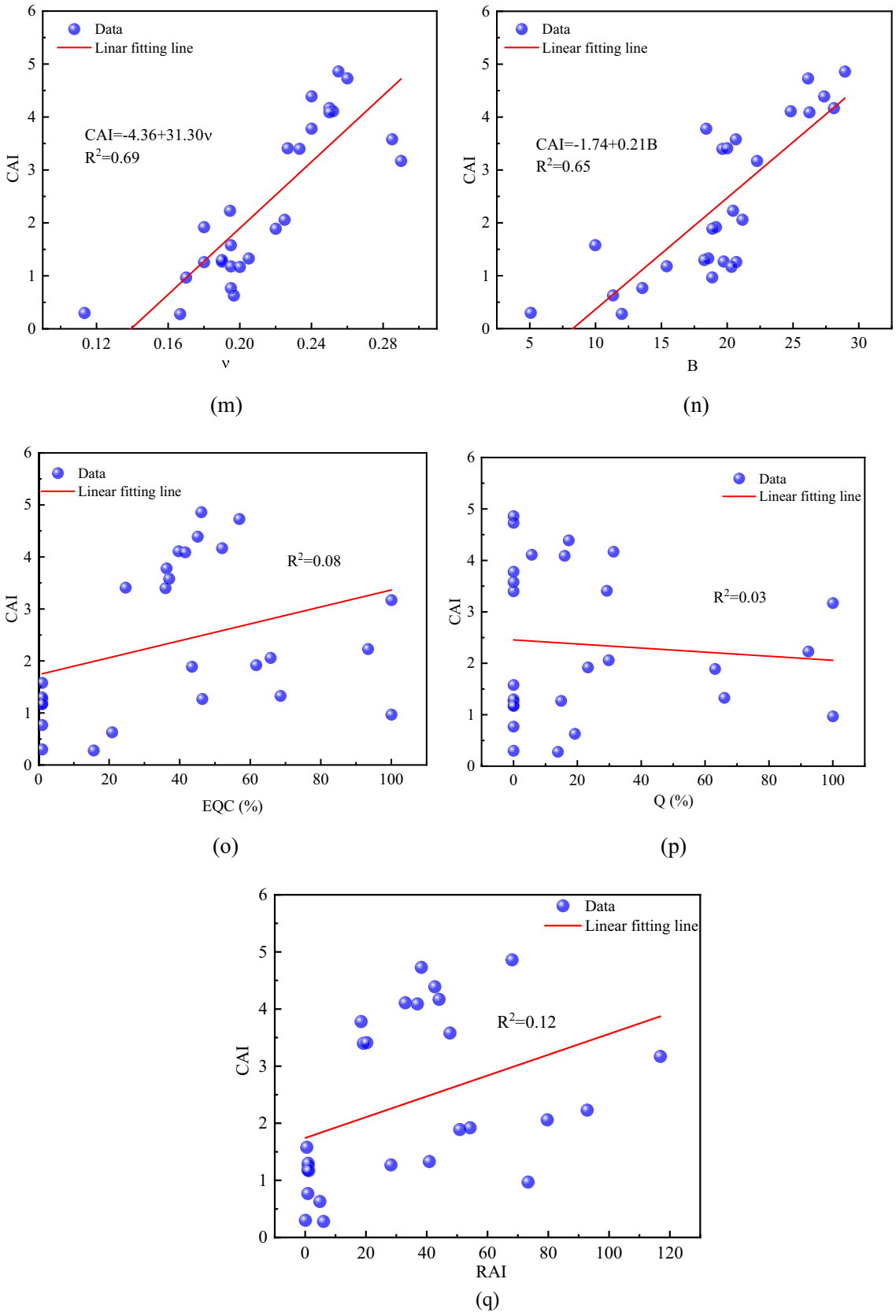

Fig. 8 (continued)

Table 8 The equations between the CAI and other parameters using simple regression

Eq.	Equations	R^2
5	CAI = 4.86–4.58/(1 + exp(11.78ρ-28.99))	0.87
6	CAI=-2.92 + 0.01 H	0.66
7	CAI = 0.28 + 4.58/(1 + exp(0.01V_s-21.36))	0.49
8	CAI=-5.14 + 0.002V_p	0.58
9	CAI = 7.43–0.91λ	0.64
10	CAI=-1.91 + 2.33D	0.73
11	CAI = 0.28 + 4.58/(1 + exp(35.71P-2.83))	0.94
12	CAI = 4.86–4.58/(1 + exp(4BTS-20.02))	0.64
13	CAI=-0.79 + 0.03UCS	0.61
14	CAI=-7.13 + 0.23φ	0.78
15	CAI=-0.27 + 0.17 C	0.70
16	CAI=-0.21 + 0.09E	0.72
17	CAI=-4.36 + 31.30ν	0.69
18	CAI=-1.74 + 0.21B	0.65

coefficient was 0.73, indicating significant linear relationships. Although there were no linear relationships between CAI and density and porosity, the Boltzmann function was established to evaluate the nonlinear fitting degree. The coefficient of determination (R^2) between CAI and density is 0.87, and the correlation is very significant. The density of rocks mainly ranges from 2.4 g/cm^3 to 2.8 g/cm^3 except for the coralreef limestone, which has a density of 1.05 g/cm^3 due to high porosity. Moreover, the coefficient of determination (R^2) between CAI and porosity is 0.94, and the correlation is significant. The porosity of coralreef limestone is 56.44%, which reduces the fitting degree.

Two types of correlations including positive linear and nonlinear correlations were summarized between CAI and mechanical properties. Specifically, the Boltzmann model, a nonlinear relationship, was established between CAI and BTS, with a coefficient of determination (R^2) of 0.64, indicating that BTS explained 64% of the variation in CAI. Moreover, CAI was positively correlated with UCS, internal friction angle, cohesion, elastic modulus, Poisson's ratio, and brittleness. In Fig. 8, the coefficient of determination (R^2) between CAI and mechanical parameters was greater than 0.8 for the linear relationships. The excellent linear fitting performance was observed between CAI and internal friction angle, while the weak linear fitting performance existed between CAI and brittleness.

There were no distinct correlations between CAI and mineralogical properties based on PCC and fitting results. It was clearly seen from Fig. 7 that there were no linear relationships between CAI and Q, EQC, and RAI. As shown in Fig. 8. EQC, RAI, and Q were dispersed, there was no appropriate model that could be used to predict the CAI. It should be noted that the linear or nonlinear models between CAI and Q, and EQC were suggested by Capik and Yilmaz (2017), Suana and Peters (1982), West (1989), and Yarali et al. (2008). They stated that Q and EQC are the important factors affecting CAI. However, Q and EQC showed a weak correlation with CAI due to varying CAI among rocks with the same mineral composition. In other words, CAI is related to not only mineral composition but also other parameters such as porosity, UCS. For all rocks, CAI is not significantly correlated with EQC and Q. However, for the same rock types, CAI is significantly correlated with EQC, because rocks of the same type are of the same genesis, with similar grain sizes and void properties, and the mineralogical compositions of the rocks have a more pronounced effect on CAI. Based on the relationships between the CAI and physio-mechanical parameters, the models were developed for the prediction of CAI using simple linear regression and the Boltzmann function (Table 8). The R^2 values of these models range from 0.49 to 0.94, with the model based on porosity showing excellent forecasting performance over other models. Although there is some certain correlation between CAI and physio-mechanical parameters, the

Table 9 The equations between the CAI and other parameters using multiregression

Eq.	Equations	R^2	Std. error of the estimate	DW	F
19	CAI = 2.883 + 0.007H + 0.001V_p-0.264λ-2.227ρ	0.878	0.514	1.56	47.74
20	CAI=-3.735-0.407BTS + 0.066φ + 0.023 C + 0.055E + 17.196ν	0.922	0.409	1.25	78.35
21	CAI = 1.627-0.039Q + 0.048RAI	0.443	1.097	0.69	11.34
22	CAI=-4.996 + 1.135D + 0.126φ + 0.002RAI	0.851	0.567	1.51	50.52
23	CAI=-4.928 + 1.228D + 0.122φ	0.856	0.558	1.56	78.24
24	CAI=-2.006 + 2.433D-0.002RAI	0.769	0.707	1.60	44.25
25	CAI=-6.248 + 0.202φ + 0.007RAI	0.811	0.640	1.27	56.69
26	CAI = 1.581 − 0.335λ + 0.533D + 0.050E + 0.005RAI	0.912	0.435	1.58	68.77

Table 10 Multivariate regression coefficients for the selected models

Coefficients[a]							
Models		Unstandardized coefficients		Standardized coefficients	t	*Sig.*	VIF
		B	Std. Error	Beta			
1	(Constant)	2.829	1.357		2.085	0.049	
	H	0.006	0.001	0.771	4.175	0.000	7.269
	V_P	0.001	0.000	0.288	2.425	0.024	2.994
	λ	-0.307	0.110	-0.307	-2.805	0.010	1.546
	ρ	-2.175	0.598	-0.508	-3.637	0.001	4.154
2	(Constant)	-3.735	0.823		-4.537	0.000	
	BTS	-0.407	0.094	-0.347	-4.336	0.000	2.147
	φ	0.066	0.030	0.278	2.167	0.041	5.516
	E	0.055	0.012	0.551	4.678	0.000	4.650
	ν	17.196	3.411	0.462	5.042	0.000	2.811
3	(Constant)	1.627	0.314		5.178	0.000	
	Q	-0.039	0.010	-0.866	-3.930	0.001	2.269
	RAI	0.048	0.010	1.042	4.727	0.000	2.269
4	(Constant)	-4.996	0.884		-5.651	0.000	
	D	1.135	0.415	0.425	2.738	0.012	4.206
	φ	0.126	0.033	0.531	3.774	0.001	3.459
	RAI	0.002	0.004	0.042	0.461	0.649	1.418
5	(Constant)	-4.928	0.857		-5.749	0.000	
	D	1.228	0.356	0.460	3.452	0.002	3.203
	φ	0.122	0.032	0.514	3.855	0.001	3.203
6	(Constant)	-2.006	0.488		-4.108	0.000	
	D	2.433	0.289	0.911	8.428	0.000	1.314
	RAI	-0.002	0.005	-0.051	-0.471	0.642	1.314
7	(Constant)	-6.248	0.853		-7.328	0.000	
	φ	0.202	0.021	0.851	9.594	0.000	1.080
	RAI	0.007	0.004	0.162	1.827	0.080	1.080
8	(Constant)	1.581	0.972		1.627	0.118	
	λ	-0.335	0.098	0.334	-3.408	0.003	2.858
	D	0.533	0.346	0.200	1.542	0.137	4.984
	E	0.050	0.010	0.497	5.147	0.000	2.772
	RAI	0.005	0.003	0.110	1.449	0.161	1.698

[a]Dependent variable: CAI

accuracy of predicting CAI by relying on a single parameter is limited.

Multi-regression

Most of the factors involving physical, mechanical, and mineralogical parameters have certain effects on CAI, which are impossible to isolate and study individually. Therefore, multiregression, a method to solve the multi-source data fusion, was calculated based on the Enter method using SPSS software. The data distribution was examined before multiregression, then the data with normal distribution was used for analysis. Notably, Durbin-Watson (DW) test is used for the purpose of testing whether the independent variables are known to be independent or not. Moreover, variance inflation factor (VIF) can characterize the covariance degree between independent variables. Also, the level of significance (*Sig*) and Fisher index (*F*) are calculated for all models. Statistically speaking, a model can be considered a better fit when the *F* is higher, $Sig < 0.05$, DW is about 2,

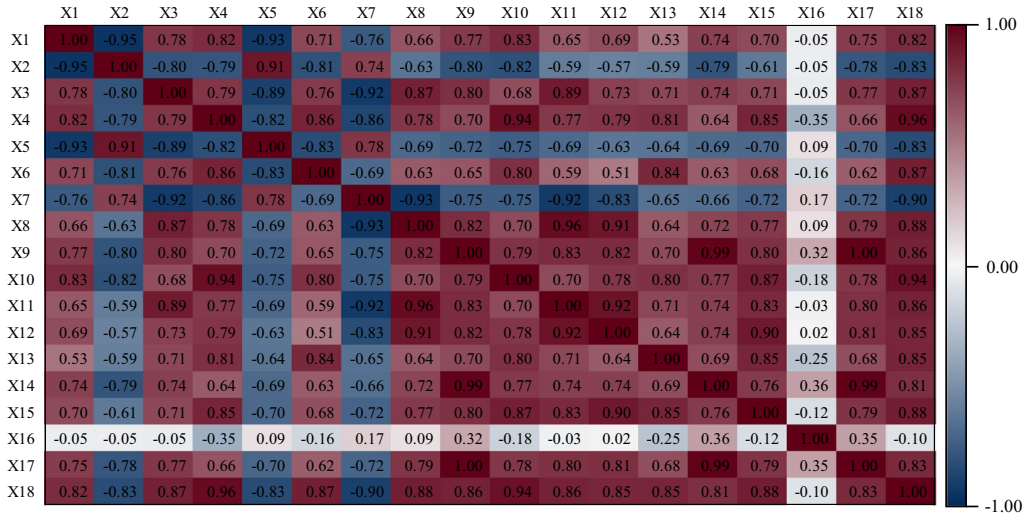

(a)

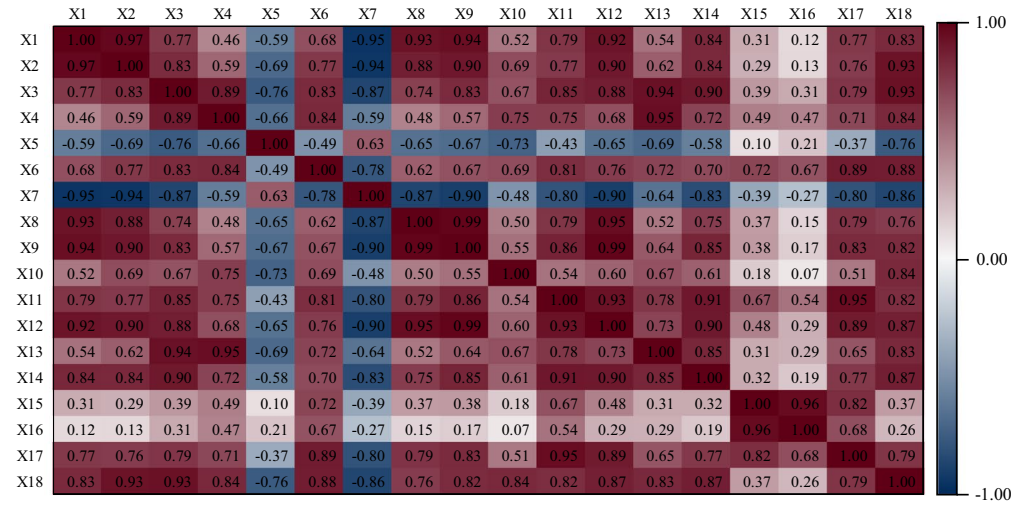

(b)

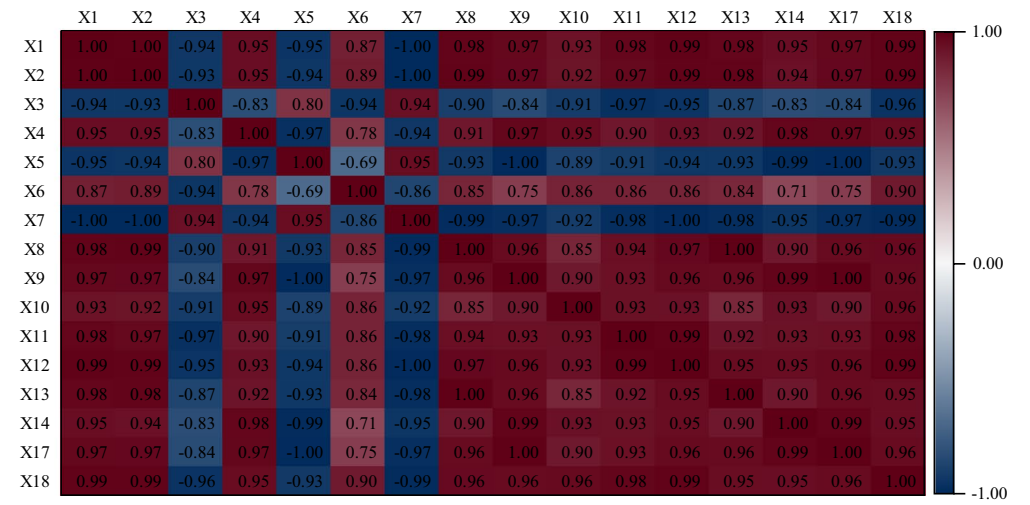

(c)

Fig. 9 Pearson correlation coefficient diagram for different rocks. **a** Granite; **b** Sandstone; **c** Limestone

Table 11 The coefficients of determination (R^2) for the linear model*

Parameters	All rocks	Granite	Sandstone	Limestone
CAI and ρ	Nonlinear	0.62	0.63	0.98
CAI and H	0.66	0.64	0.83	0.97
CAI and V_S	Nonlinear	0.71	0.85	0.89
CAI and V_P	0.58	0.90	0.65	0.87
CAI and λ	0.64	0.65	0.50	0.82
CAI and D	0.73	0.72	0.73	0.74
CAI and P	Nonlinear	0.77	0.70	0.97
CAI and BTS	Nonlinear	0.73	0.50	0.89
CAI and UCS	0.61	0.70	0.62	0.89
CAI and φ	0.78	0.86	0.65	0.90
CAI and C	0.70	0.66	0.60	0.96
CAI and E	0.72	0.67	0.71	0.98
CAI and ν	0.69	0.68	0.64	0.87
CAI and B	0.65	0.59	0.72	0.86
CAI and EQC	No relation	0.74	0.63	/
CAI and Q	No relation	No relation	No relation	/
CAI and RAI	No relation	0.64	0.90	/

*Nonlinear indicates that other models were used to predict; No relation indicates that there is no significant relationship between the CAI and other parameters; / indicates that it is unnecessary to establish the correlation; the number is the R^2 for the linear model

and VIF < 10. A model is considered not to be statistically significant if $Sig > 0.05$.

Table 9 shows the eight models selected for determining CAI. Multiple regression analysis was carried out to specify whether CAI can be best estimated by one specific factor or by a combination of rock parameters. The relationships between CAI and rock physical, mechanical and mineralogical properties were established, respectively. Leeb hardness, longitudinal wave velocity, thermal conductivity, and density were perfectly determined to establish the relationship between CAI and physical parameters. An R^2 value of 0.878 and a DW of 1.56 were calculated, indicating that the model was better. The mechanical parameters including BTS, internal friction angle, cohesion, elastic modulus, and Poisson's ratio were determined to forecast CAI. The R^2 value of 0.922 was maximum in the established eight models. Then Q and RAI were selected to predict the CAI from the mineralogical aspect. Mineral-based derived model has a smaller R^2 value than models based on rock physical and mechanical parameters. One parameter form each of the mineralogical, physical, and mechanical parameters was selected to predict the CAI. The best model developed by the diffusion coefficient, internal friction angle, and RAI had the R^2 value of 0.851. Moreover, two aspects of rock parameters were used to predict CAI. Specifically, the diffusion coefficient (physical) and internal friction angle (mechanical) were used to estimate CAI, the diffusion coefficient (physical) and RAI (mineralogical) were used to estimate CAI, the internal friction angle (mechanical) and RAI (mineralogical) were used to estimate CAI. Notably, four parameters with the maximum PCC value were used to predict CAI, as a result, a high R^2 value of 0.912 was calculated. Multivariate regression coefficients were shown in Table 10. It was suggested that these models were basically satisfactory based on the results of *Sig* and VIF values. Generally speaking, the best model developed for the prediction of CAI was derived based on the rock mechanical parameters.

Discussion

The relationships between CAI and 14 parameters including physical and mechanical properties were primarily acquired using simple regression. Notably, the predictive performance of all simple models in terms of all rocks is not quite satisfactory. Moreover, it is hard to forecast CAI through mineralogical properties. More rock types increase the uncertainties of rock properties, so the correlation between CAI and single parameter is not high. In order to reduce the uncertainty caused by rock type, simple regression for the same rock was carried out. Figure 9 represented the PCC results of different rocks including granite, sandstone, and limestone. Statistically speaking, the PCC value acquired from the same rock type increased slightly compared to the PCC results derived in Section 3.1. In other words, the significance of linear correlations between CAI and other parameters increased for the same rock type. As an example, the PCC value between CAI and longitudinal wave velocity was 0.81, while it increased to 0.96 for granite, 0.84 for sandstone, and 0.95 for limestone. Notably, some rock parameters showed a different linear relationship with the CAI compared with the PCC value in Section 3.1. To be specific, the transverse wave velocity showed a negative linear correlation with CAI based on all rocks, but a positive linear correlation with CAI for the granite and sandstone. Therefore, it is suggested that the correlation should be identified based on the classification of rocks.

Furthermore, the R^2 values for the linear model between CAI and 17 rock parameters were calculated, as shown in Table 11. It was concluded that three correlations including nonlinear, linear, and no relation appeared for all rocks, notably, there was no relation between CAI and rock mineralogical parameters. After the classification of rock types, the R^2 value increased significantly or remained stable in terms of some rock physical and mechanical parameters. Moreover, the nonlinear correlation changed into significant linear correlation for density, transverse wave velocity, porosity, and BTS. An interesting phenomenon on the mineralogical parameters occurred. Concretely, after the classification of rock types, CAI showed a linear correlation with EQC and RAI for the granite and sandstone, Q still showed no relation

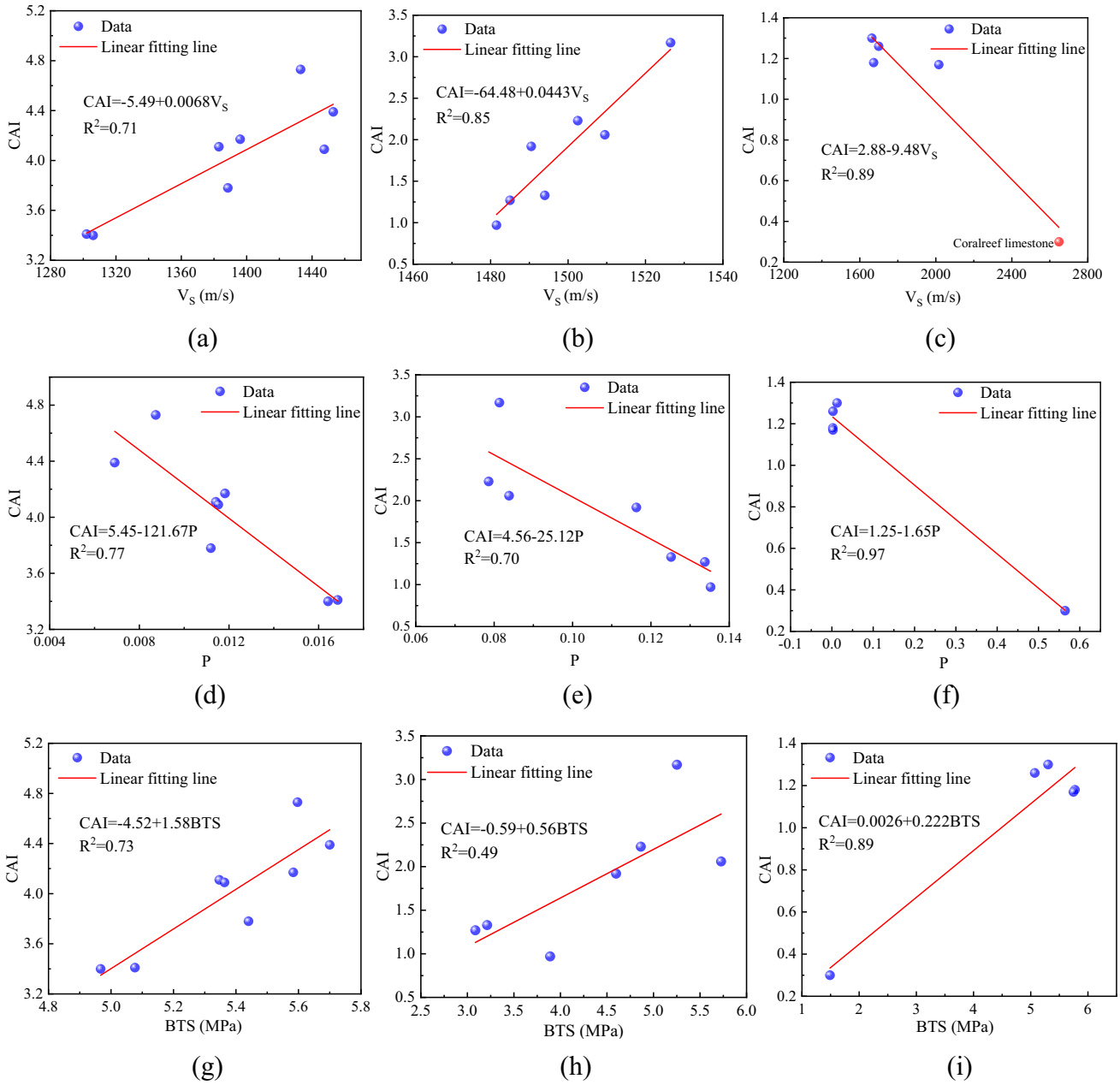

Fig. 10 The relationships between the CAI and physical and mechanical properties. **a** CAI and V_S for the granite; **b** CAI and V_S for the sandstone; **c** CAI and V_S for the limestone; **d** CAI and P for the granite; **e** CAI and P for the sandstone; **f** CAI and P for the limestone; **g** CAI and BTS for the granite; **h** CAI and BTS for the sandstone; **i** CAI and BTS for the limestone

with CAI. It means that EQC can excellently characterize CAI for the granite and sandstone, the other mineral compositions except for the quartz also have a significant effect on CAI. However, a special phenomenon between CAI and mineralogical parameters occurred for the limestone. Due to that the limestone merely included the calcite not quartz, Q and EQC were the same for five limestones. From my perspective, EQC is unfit to characterize CAI for the monomineralogic rock especially the limestone, which only includes the calcite or aragonite.

Some typical correlations, especially the transition from nonlinear to linear correlations, were selected for specific analysis. As shown in Fig. 10, the porosity and BTS showed a similar linear trend for the three rock types, while transverse wave velocity was positively correlated for the granite and sandstone and negatively correlated for the limestone with CAI. Therefore, it is paradoxical to characterize CAI

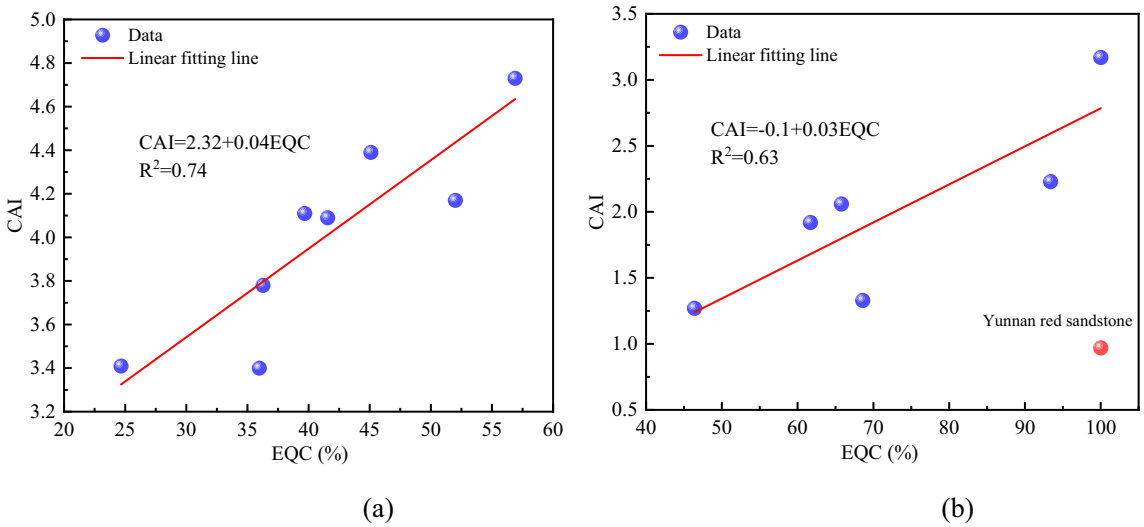

Fig. 11 The relationships between the CAI and mineralogical properties. **a** CAI and EQC for the granite; **b** CAI and EQC for the sandstone

using transverse wave velocity for different rocks. Furthermore, the positive linear relationship between CAI and EQC for the granite and sandstone was represented in Fig. 11. Notably, EQC of Yunnan red sandstone deviated from the fitting line. However, Yunnan beige sandstone with the same mineral composition as Yunnan red sandstone has greater abrasiveness. Therefore, some obvious reasons for this phenomenon are related to the fact that the grain size is small based on the petrographic observation in Fig. 5.

Based on the multiregression analysis, it was concluded that the model established by mechanical parameters had an excellent performance of predicting CAI. Moreover, the multiple regression models had a higher R^2 value than the simple models, indicating that the predictive performance on CAI increased for the multiple regression models. However, rock mechanical tests are time-consuming, costly, and destructive to the rock, the acquisition of rock mechanical parameters is demanding. The rock physical tests are rapid, inexpensive, and non-destructive to the rock. Therefore, Eq. (26) seems more appropriate for predicting CAI after consideration of the simplicity and period of testing methods.

Conclusions

Rock abrasiveness is an important factor affecting tool wear in rock excavation. Based on 27 groups of sedimentary, igneous, and metamorphic rocks from China, single-factor and multiregression software were used to investigate the correlations between CAI and physical, mechanical, and mineralogical properties in this paper. The following conclusions are obtained:

(1) Based on laboratory test methods, seven physical parameters, seven mechanical parameters, three mineralogical parameters, and CAI were measured and calculated. The petrographic observation was performed to intensify the understanding of variation of CAI. The PCC value was acquired to primarily investigate the linear correlation and provide the reference for the simple regression and multiregression.

(2) Linear and Boltzmann models were acquired based on the simple regression. The results show that CAI increases with increasing density, leeb hardness, longitudinal wave velocity, diffusion coefficient, BTS, UCS, internal friction angle, cohesion, E, Poisson' ratio, and brittleness, while decreases with increasing transverse wave velocity, thermal conductivity, porosity. Moreover, there were no distinct relationships between CAI and mineralogical properties. The fitting coefficient of CAI and porosity was 0.94.

(3) Through the analysis of the R^2 value, a better multiregression model ($R^2 = 0.92$) based on the mechanical parameters was obtained. However, a more feasible model ($R2 = 0.91$) based on the thermal conductivity, diffusion coefficient, elastic modulus, and RAI was also suggested after consideration of the simplicity and period of parameter measurement.

(4) After the classification of rock types, the R^2 value increased significantly or remained stable in terms of some rock physical and mechanical parameters, CAI showed a linear correlation with EQC and RAI for the granite and sandstone, Q still showed no relation with CAI. EQC is unfit to characterize CAI for the monomineralogic rock.

Acknowledgements This research is supported by the Jiangsu Excellent Postdoctoral Program (2022ZB509), the National Natural Science Foundation of China (No. 42307244 and 42230704), and the Xuzhou Science and Technology Plan Social Development Key Special Project (SHFZZDZX20210017).

Data availability Data will be made available on request.

Declarations

Conflict of interest The authors declare that they have no conflict of interest.

References

Alber M, Yarali O, Dahl F, Bruland A, Kasling H, Michalakopoulos TN, Cardu M, Hagan P, Aydin H, Ozarslan A (2014) ISRM suggested method for determining the abrasivity of rock by the CERCHAR abrasivity test. Rock Mech Rock Eng 47(1):261–266

ASTM (2010) Standard test method for compressive strength and elastic moduli of intact rock core specimens under varying states of stress and temperatures. American Standarts for Testing and Materials, D7012-04, USA

Capik M, Yilmaz AO (2017) Correlation between Cerchar abrasivity index, rock properties, and drill bit lifetime. Arab J Geosci 10(1):1–12

Deliormanli AH (2012) Cerchar abrasivity index (CAI) and its relation to strength and abrasion test methods for marble stones. Constr Build Mater 30:16–21

Deng LC, Zhang FB, Li XZ, Zhang C, Ji YK, Wu Y (2022a) Experimental and numerical investigations on rock breaking of TBM disc cutter based on a novel platform with rotational cutting. Rock Mech Rock Eng 56(2):1415–1436

Deng LC, Li XZ, Chen YW, Zhuang QW, Zhu LH, Zhang C (2022b) Investigations on cutting force and temperature field of pick cutter based on single factor and orthogonal test methods. Rock Mech Rock Eng 56(1):619–645

Deng LC, Zhang C, Zhuang QW, Li XZ, Yuan YX (2022c) Development and application of a full-scale mechanical rock-cutting platform for measuring the cutting performance of TBM cutter. Measurement 204:112036

Er S, Tuğrul A (2016) Correlation of physico-mechanical properties of granitic rocks with Cerchar Abrasivity Index in Turkey. Measurement 91:114–123

He JM, Li SD, Li X, Wang X, Guo JY (2016) Study on the correlations between abrasiveness and mechanical properties of rocks combining with the microstructure characteristic. Rock Mech Rock Eng 49(7):2945–2951

Hucka V, Das B (1974) Brittleness determination of rocks by different methods. Int J Rock Mech Min Sci Geomech Abst Pergamon 11(10):389–392

ISRM (1979) Suggested method for determining the uniaxial compressive strength and deformability of rock materials. Int J Rock Mech Min Sci 16:135–140

Ko TY, Kim TK, Son Y, Jeon S (2016) Effect of geomechanical properties on Cerchar Abrasivity Index (CAI) and its application to TBM tunnelling. Tunn Undergr Space Technol 57:99–111

Li SJ, Kuang ZH, Qiu SL (2022) Review of rock brittleness evaluation methods and discussion on their adaptabilities. J Eng Geol 30(1):59–70

Liu W, Liu XJ, Ding Y, Xiong J, Liang LX (2023) The investigation on shale mechanical characteristics and brittleness evaluation. Sci Rep 13(1):22936

Majeed Y, Abu Bakar MZ (2016) Statistical evaluation of CERCHAR Abrasivity Index (CAI) measurement methods and dependence on petrographic and mechanical properties of selected rocks of Pakistan. Bull Eng Geol Environ 75(3):1341–1360

Moradizadeh M, Cheshomi A, Ghafoori M, TrighAzali S (2016) Correlation of equivalent quartz content, slake durability index and Is_{50} with Cerchar abrasiveness index for different types of rock. Int J Rock Mech Min Sci 86:42–47

Moradizadeh M, Ghafoori M, Lashkaripour G, Tarigh Azali S (2013) Utilizing geological properties for predicting Cerchar abrasiveness index (CAI) in sandstones. Int J Emerg Technol Adv Eng 3(9):99–109

Ozdogan MV, Deliormanli AH, Yenice H (2018) The correlations between the Cerchar abrasivity index and the geomechanical properties of building stones. Arab J Geosci 11(20):604

Rostami J, Ghasemi A, Gharahbagh EA, Dogruoz C, Dahl F (2014) Study of dominant factors affecting Cerchar abrasivity index. Rock Mech Rock Eng 47(5):1905–1919

Suana M, Peters TJ (1982) The Cerchar abrasivity index and its relation to rock mineralogy and petrography. Rock Mech Rock Eng 15(1):1–8

Sun JD, Shang Y, Wang K, Wang CH, Ma F, Sun CY (2023) A new prediction model for disc cutter wear based on Cerchar Abrasivity Index. Wear 526–527:204927

Thuro K, Plinninger RJ (2003) Hard rock tunnel boring, cutting, drilling and blasting: rock parameters for excavatability. In: ISRM, 2003 Technology roadmap for rock mechanics, South African Institute of Mining and Metallurgy, pp 1227–1234

Tian X, Su GY (2023) Correlation analysis between fault frequency and service time of underground fluid instruments. Geod Geodyn 14(4):411–418

Torrijo FJ, Garzón-Roca J, Company J, Cobos G (2018) Estimation of Cerchar abrasivity index of andesitic rocks in Ecuador from chemical compounds and petrographical properties using regression analyses. Bull Eng Geol Environ 78(4):2331–2344

Ulusay R (ed) (2015) The ISRM suggested methods for rock characterization, testing and monitoring: 2007–2014 Cham. Springer, Switzerland

Wang LH, Li HP, Zhao XJ, Zhang Q (2017) Development of a prediction model for the wear evolution of disc cutters on rock TBM cutterhead. Tunn Undergr Space Technol 67:147–157

West G (1989) Rock abrasiveness testing for tunnelling. Int J Rock Mech Min Sci 26:151–160

Yaralı O, Yaşar E, Bacak G, Ranjith PG (2008) A study of rock abrasivity and tool wear in coal measures rocks. Coal Geol 74(1):53–66

Yu HG, Tao JF, Huang S, Qin CJ, Xiao DY, Liu CL (2021) A field parameters-based method for real-time wear estimation of disc cutter on TBM cutterhead. Autom Constr 124:103603

Zhang GZ, Konietzky H, Frühwirt T (2020) Investigation of scratching specific energy in the Cerchar abrasivity test and its application for evaluating rock-tool interaction and efficiency of rock cutting. Wear 448:203218

Zhang SR, She L, Wang C, Wang YJ, Cao RL, Li YL, Cao KL (2021) Investigation on the relationship among the Cerchar abrasivity index, drilling parameters and physical and mechanical properties of the rock. Tunn Undergr Space Technol 112:103907